Molecular Biology of the Cell
Vol. 20, 3725–3739, August 15, 2009

α-Synuclein and Its A30P Mutant Affect Actin Cytoskeletal Structure and Dynamics

Vítor L. Sousa,*†‡§ Serena Bellani,†§ Maila Giannandrea,† Malikmohamed Yousuf,† Flavia Valtorta,*†‖ Jacopo Meldolesi,*†‖ and Evelina Chieregatti*†¶

*Department of Neuroscience, San Raffaele Scientific Institute, †San Raffaele Vita-Salute University, ‖IIT Research Unit of Molecular Neuroscience, and Istituto Nazionale di Neuroscienze, 20132 Milan, Italy; and ¶Department of Neuroscience and Brain Technology, The Italian Institute of Technology, 16163 Genoa, Italy

Submitted March 20, 2008; Revised June 12, 2009; Accepted June 15, 2009
Monitoring Editor: Josephine C. Adams

The function of α-synuclein, a soluble protein abundant in the brain and concentrated at presynaptic terminals, is still undefined. Yet, α-synuclein overexpression and the expression of its A30P mutant are associated with familial Parkinson's disease. Working in cell-free conditions, in two cell lines as well as in primary neurons we demonstrate that α-synuclein and its A30P mutant have different effects on actin polymerization. Wild-type α-synuclein binds actin, slows down its polymerization and accelerates its depolymerization, probably by monomer sequestration; A30P mutant α-synuclein increases the rate of actin polymerization and disrupts the cytoskeleton during reassembly of actin filaments. Consequently, in cells expressing mutant α-synuclein, cytoskeleton-dependent processes, such as cell migration, are inhibited, while exo- and endocytic traffic is altered. In hippocampal neurons from mice carrying a deletion of the α-synuclein gene, electroporation of wild-type α-synuclein increases actin instability during remodeling, with growth of lamellipodia-like structures and apparent cell enlargement, whereas A30P α-synuclein induces discrete actin-rich foci during cytoskeleton reassembly. In conclusion, α-synuclein appears to play a major role in actin cytoskeletal dynamics and various aspects of microfilament function. Actin cytoskeletal disruption induced by the A30P mutant might alter various cellular processes and thereby play a role in the pathogenesis of neurodegeneration.

INTRODUCTION

During the progression of Parkinson's disease (PD), the dopaminergic neurons of the substantia nigra, pars compacta accumulate proteinaceous inclusion bodies, the Lewy bodies (Dawson and Dawson, 2003) before undergoing degeneration. The main component of these bodies, α-synuclein, is a 14-kDa soluble, intrinsically unfolded protein (Weinreb *et al.*, 1996; Uversky, 2003) which is expressed in all neurons and enriched at many synaptic terminals (Totterdell *et al.*, 2004). Various mutations of the α-synuclein coding gene, in particular the Ala30Pro (A30P) mutation (Kruger *et al.*, 1998) and the duplication/triplication of the region of chromosome (4q21) spanning the α-synuclein gene (Singleton *et al.*, 2003), trigger the onset of autosomal dominant forms of PD in several pedigrees. In addition, α-synuclein appears to be involved in the pathogenesis of the sporadic forms of the disease.

In the presynaptic compartment α-synuclein has been proposed to participate both in the exocytic process (Chandra *et al.*, 2005) and in the regulation of the synaptic vesicle pools. However, conflicting results have been reported in the knock-out mice. Depletion of the reserve pool of synaptic vesicles has been reported by one group (Cabin *et al.*, 2002) but not by another (Chandra *et al.*, 2004). Likewise, transmitter release from neurosecretory cells has been reported to be modulated by α-synuclein, either in a positive (Liu *et al.*, 2004) or in a negative manner (Larsen *et al.*, 2006). In addition, α-synuclein has been suggested to play a role in neurite outgrowth (Takenouchi *et al.*, 2001) and in the adhesion of brain-derived cells (Takenouchi *et al.*, 2001; Tsuboi *et al.*, 2005). Interactions of α-synuclein have been reported with phospholipid bilayers and with a variety of proteins: synphilyn, 14-3-3 proteins, various PKC isoforms, MAPK, α- and β-tubulin, and tau (Lucking and Brice, 2000). Whether any of these proteins acts as a mediator of the physiological or pathological actions of α-synuclein is still unknown.

A protein known to play a critical role in neurosecretion (Dillon and Goda, 2005), that may participate in α-synuclein action is actin. Actin filaments are involved in the transport of clear and dense-core vesicles along the axon and in their clustering at the plasma membrane sites where exocytosis takes place. Moreover, actin fibers form a dense filamentous network beneath the plasma membrane, which is reorganized upon cell stimulation to allow the access of vesicles to fusion sites. Rapid remodeling of the actin cytoskeleton is also required for cell adhesion and neurite outgrowth. So far

This article was published online ahead of print in *MBC in Press* (http://www.molbiolcell.org/cgi/doi/10.1091/mbc.E08-03-0302) on June 24, 2009.

§ These authors contributed equally to this work.

‡ Present address: Areta International s.r.l., 21040 Gerenzano, Italy.

Address correspondence to: Evelina Chieregatti (evelina.chieregatti@iit.it).

Abbreviations used: FITC, fluorescein isothiocyanate; IPTG, isopropyl β-D-1-thiogalactopyranoside; LatA, latrunculin A; MDCK, Madin-Darby canine kidney; N2A, Neuro2a; PD, Parkinson's disease; SLO, streptolysin-O; wt, wild type.

the possible interaction of α-synuclein and actin has not been studied in depth. The two proteins have been observed to partially colocalize in two neuronal cell lines (Esposito *et al.*, 2007): actin levels are altered in *Drosophila melanogaster* and in *Caenorhabditis elegans* models of PD (Xun *et al.*, 2007; Ichibangase *et al.*, 2008), and actin is present in the cytoplasmic α-synuclein aggregates induced by rotenone in dopaminergic neurons (Zhou *et al.*, 2004). Recently α-synuclein has been shown to activate the protein phosphatase 2A (Peng *et al.*, 2005), a phosphatase involved in actin dephosphorylation.

In the present work the interaction of wild-type (wt) α-synuclein and of its A30P mutant with actin has been investigated in a variety of experimental models. The results indicate that wt α-synuclein has a role in the regulation of actin dynamics, and that this role is profoundly changed by the A30P mutation. We hypothesize that the α-synuclein–induced alterations of the actin cytoskeleton, with ensuing changes of synaptic function, could ultimately play a role in the pathogenesis of PD.

MATERIALS AND METHODS

Reagents

Cell culture media and solutions were from BioWhittaker (Walkersville, MD), Opti-MEM medium was from Invitrogen-Invitrogen (Carlsbad, CA) and FetalClone III (FCIII) was from Euroclone (Paignton, United Kingdom). Isopropyl β-D-1-thiogalactopyranoside (IPTG) was from Sigma-Aldrich (St. Louis, MO), latrunculin A (LatA), fluorescein isothiocyanate (FITC)-coupled phalloidin, pyrene-iodoacetamide and FM4-64-FX were from Invitrogen-Molecular Probes (Carlsbad, CA). Recombinant human plasma gelsolin was from Cytoskeleton (Denver, CO), and cytochalasin D was from Calbiochem (La Jolla, CA). The following antibodies were used: monoclonal anti-actin, anti-β-tubulin (Sigma-Aldrich) and anti-α-synuclein (BD Transduction Laboratories, Franklin Lakes, NJ); rabbit polyclonal anti-actin (Sigma), and anti-phosphoserine (Abcam, Cambridge, MA).

Cell Culture

Murine neuroblastoma Neuro2A (N2A) cells were grown in DMEM supplemented with 10% FCIII, 1% Ultraglutamine, 1% penicillin and streptomycin, and 20 mM HEPES, pH 7.2, at 37°C in a 5% CO_2 incubator. Madin-Darby canine kidney (MDCK) cells were grown in DMEM supplemented with 5% FCIII, 1% Ultraglutamine, and 1% penicillin and streptomycin. N2A stably transfected clones were selected with 1 mg/ml geneticin (Calbiochem). Transfections were performed with Lipofectamine 2000 (Invitrogen) according to the manufacturer's instructions. The DNA fragments coding for human wt and A30P α-synucleins including the stop codon were inserted into the pEGFP-N1 vector for transfection in N2A cells. The same DNA fragments were inserted in pOPRSVI-1 vector (Cheong *et al.*, 1999). The resulting constructs were transfected into MDCK cells expressing the *lac* repressor (McCarthy *et al.*, 1996). The vector and clones were gifts from Dr. D. Zacchetti (San Raffaele Scientific Institute, Milan, Italy).

Primary neuronal cultures were prepared from the hippocampi of C57BL/6J OlaHsd (C57BL/6S) mouse embryos (Harlan, Milan, Italy) at embryonic day 18 (E18) as previously described (Banker and Cowan, 1977). This substrain of C57BL/6J mice is known to carry a chromosomal deletion encompassing the α-synuclein locus gene (Snca; Specht and Schoepfer, 2001).

Primary hippocampal neurons were electroporated by Amaxa Nucleofector technology (Amaxa Biosystems, Cologne, Germany) immediately after dissociation (Gartner *et al.*, 2006) with the same wt or A30P α-synucleins cDNA used for N2A cell transfection and were plated on glass coverslips at a density of 10,000 cells/cm^2. Four hours after plating, coverslips were placed in a clean dish containing glia-conditioned medium: MEM supplemented with 1% N2 supplement (Invitrogen-Invitrogen), 2 mM glutamine (BioWhittaker), 1 mM sodium pyruvate (Sigma-Aldrich), and 4 mM glucose.

α-Synuclein Purification

Constructs encoding the full-length human wt and A30P α-synucleins inserted in the pET21d plasmid were a kind gift from Dr. B. Lauring (Columbia University, New York). Purification was performed as previously described (Martinez *et al.*, 2003). Bacteria were induced during the exponential phase with 0.4 mM IPTG for 2 h, harvested by centrifugation, and washed twice with cold phosphate-buffered saline (PBS). The pellet was resuspended in 20 mM HEPES/KOH, pH 7.2, 100 mM KCl and heated for 5 min at 90°C. The cell lysate was centrifuged at 72,000 × *g* for 30 min, and the supernatant was loaded on a HiTrap monoQ column (GE Healthcare, Uppsala, Sweden). α-Synuclein was eluted with a liner gradient of KCl from 100 to 500 mM, and the fractions of interest were concentrated on Centricon (Millipore, Billerica, MA) before loading on a Superose 12 column (GE Healthcare). The fractions containing α-synuclein were pooled and stored at −80°C.

Actin Polymerization Assays

Actin was purified from rabbit muscle as in Spudich and Watt (1971) and MacLean-Fletcher and Pollard (1980). Aliquots were frozen in liquid nitrogen and centrifuged at 355,000 × *g* before every experiment. Polymerization kinetics assays were performed with 5 μM actin (5% pyrenylated) as described in Chieregatti *et al.* (1996), in G buffer (2 mM Tris/HCl pH 8.0, 0.2 mM $CaCl_2$, 0.2 mM NaATP, and 0.5 mM β-mercaptoethanol). [Ca^{2+}] in the assay was adjusted with EGTA (MaxChelator v2.5 program, http://www.stanford.edu/~ cpatton/). Polymerization was initiated with 30 mM KCl, 1 mM $MgCl_2$, and either 15 or 85 mM NaCl (final concentrations). Recombinant α-synucleins were added with the salts. For depolymerization experiments actin was polymerized as above for 1 h. Depolymerization was initiated by diluting polymerized actin 1:10 or 1:50 in G buffer. Recombinant α-synucleins or α-synuclein buffer were added with the diluting G buffer, reaching a final concentration of KCl of 14 mM. Fluorescence was monitored in a Perkin Elmer-Cetus fluorometer (Monza, Italy) at 30°C (excitation at 365 nm, emission at 407 nm, 10-nm slit width). The rates of polymerization or depolymerization were calculated with the Perkin Elmer-Cetus FL WinLab software.

For the severing experiments actin was polymerized as above for 1 h, and then incubated with gelsolin, cytochalasin D, or recombinant α-synucleins, either alone or in the presence of cytochalasin D. After a 1-h incubation the samples were centrifuged at 135,000 × *g* for 20 min. Pellets and supernatants were analyzed by Coomassie blue staining of SDS gels.

For morphological analysis, actin was polymerized at a concentration of 5 μM with 100 nM free [Ca^{2+}] in the absence or presence of α-synucleins, diluted to 0.5 μM in polymerization buffer, and put on glass coverslips coated with poly-L-ornithine. Alternatively, undiluted actin was seeded on carbon-coated copper grids at room temperature for 30 min. For fluorescence analysis, coverslips were fixed with 4% paraformaldehyde (PFA), and actin fibers were labeled with FITC-phalloidin. For electron microscopy analysis, grids were washed twice with water and incubated with a saturated solution of uranyl acetate for 5 min. Samples were photographed in a Zeiss Axioplan2 microscope with a 63× Zeiss objective lens (NA 1.4) coupled with a Zeiss AxioCam HRc or in a Zeiss Leo 912AB electron microscope (Zeiss, Oberkochen, Germany). Fiber length was calculated with the Neuron J plugin (Meijering *et al.*, 2004) using the Image J program (Rasband, W.S., NIH, Bethesda, MA; http://rsb.info.nih.gov/ij/).

For sedimentation experiments, actin and α-synucleins were precleared at 130,000 × *g* for 20 min, and polymerization was performed as for the kinetic assays. After a 30-min incubation, samples were centrifuged at 15,000 × *g* for 15 min, and the supernatant was further centrifuged at 135,000 × *g* for 20 min. Pellets from both centrifugations, washed twice with the polymerization buffer, were analyzed by Western blotting together with one-half of the supernatants.

Protein Delivery with Streptolysin-O

N2A cells, grown in complete medium in 10-cm Petri dishes up to 80% confluence, were detached by pipetting and centrifuged at 20 × *g* for 5 min at 4°C. Cells were washed twice with Hanks' balanced salt solution (HBSS), resuspended in 500 μl HBSS containing 0.5 μg/ml streptolysin-O (SLO; Dr. S. Bhakdi, Mainz, Germany) and incubated for 30 min at 4°C with occasional shaking in Eppendorf tubes previously coated with 1% (wt/vol) bovine serum albumin (BSA). Cells were then centrifuged, washed three times with HBSS, and incubated for 30 min at 37°C with 12 μM α-synucleins on a thermo block with continuous agitation at 700 rpm. Cells were pelleted and incubated for 1 h at 37°C in complete medium to allow membrane resealing. Cells were plated on glass coverslips or on Petri dishes, left in the incubator, and processed for immunofluorescence or Western blot 24 h later.

Estimation of Cellular α-Synuclein Concentration

Transiently or stably transfected N2A cells and MDCK cells after 48-h induction with IPTG were resuspended in PBS, and the cellular and nuclear diameters were measured under a microscope. The cytoplasm volume was calculated subtracting the nucleus volume from the total cell volume, assuming spherical shapes. Cells were washed with PBS, homogenized in 50 mM HEPES, pH 7.2, 150 mM NaCl, 5 mM EDTA, 10% glycerol, 1% Triton X-100, and centrifuged at 15,000 × *g* to eliminate the nuclei. α-Synuclein levels in cellular post nuclear supernatant (PNS) from a known number of cells were quantified, interpolated in a standard curve of purified α-synuclein, and divided by the total cytoplasm volume.

Immunofluorescence

Cells were grown on glass coverslips, washed in PBS, fixed for 15 min with 4% PFA, and permeabilized in 0.1% Triton X-100 for 15 min. After 1-h blocking with 1% BSA, cells were incubated with primary antibodies and, after washing with PBS, cells were incubated with the secondary antibodies

and mounted with Shandon Immu-Mount (Thermo Scientific, Rockford, IL). Hippocampal neurons grown on glass coverslips were fixed in 4% PFA solution, containing 120 mM phosphate buffer, pH 7.4, and 4% sucrose. After washing with PBS, cells were incubated with primary antibodies, followed by secondary antibodies, in goat serum dilution buffer (GSDB: 15% goat serum, 450 mM NaCl, 0.1% Triton X-100, and 20 mM sodium phosphate buffer, pH 7.4). Coverslips were mounted in Airvol, and images were acquired in a Leica SP2 confocal microscope, using a Leica 63× objective lens (NA 1.4; Leica Geosystem, Eresing, Germany).

LatA Treatment and Recovery

MDCK clones were induced for 48 h with 5 mM IPTG for expression of wt or A30P α-synucleins. Depolymerization of the actin cytoskeleton was performed by incubating the cells with 5 μM LatA for 3, 5, or 10 min at 37°C. Cells were then washed, incubated in complete medium for 0, 10, 20, 40, or 60 min and processed for immunofluorescence. The same protocol was used for stably transfected N2A clones. After 2 d in culture (DIV), hippocampal neurons were treated with 1 μM LatA for 1 h at 37°C in hippocampal-conditioned medium and, after the drug wash out, the recovery of the actin cytoskeleton was followed for up to 2 h. The quantifications for neuronal culture experiments were made using a custom-made macro in ImageJ. A common threshold was applied to all images in order to exclude background fluorescence. The cell body area was evaluated as the surface defined by the neuronal outline after decoration with phalloidin. F-actin foci were counted with the "Analyze Particles" function after binary conversion and despeckling of the images. The number of foci was normalized for the number of neurons. Results were analyzed using Student's *t* test and were expressed as mean ± SD; $p < 0.05$ was considered to be significant.

Immunoprecipitation and Subcellular Fractionation

MDCK cells were lysed in immunoprecipitation (IP) buffer (50 mM HEPES, pH 7.2, 150 mM NaCl, 5 mM EDTA, and 1% Triton X-100), cleared at 300 × *g* for 5 min at 4°C, or further centrifuged at 355,000 × *g* for 30 min in a TLA 100 Beckman ultracentrifuge (Palo Alto, CA) to obtain a final supernatant. Nonfat dry milk (3% final concentration) was added to the homogenates or the final supernatants, and the samples were incubated for 2 h with protein G-Sepharose beads (Thermo Electro-Pierce, Rockford, IL) previously coated in 1% BSA, either alone or coupled to anti-α-synuclein or anti-actin antibody. The incubation was carried out at 4°C on a rotating wheel. Beads were washed with IP buffer containing 500 mM NaCl. A rat brain homogenate, prepared in a bounce homogenizer in 0.32 M sucrose, 20 mM HEPES, pH 7.2, 5 mM EGTA, and 10 mg of total protein was diluted fourfold in 20 mM HEPES, 5 mM EGTA, incubated with 1% Triton X-100 for 5 min on ice and centrifuged at 300 × *g* to remove the nuclei. The PNS was centrifuged at 355,000 × *g* for 40 min. The final supernatant, supplemented with 3% dry milk and $CaCl_2$ to obtain a $[Ca^{2+}]$ of 100 nM, was then incubated for 2 h at 4°C on a rotating wheel with protein G-Sepharose beads coupled with the affinity-purified anti-actin antibody. As control samples, either beads alone or beads incubated with the preadsorbed anti-actin antibody were used. Beads were washed as above. For fractionation experiments both the pellet and the final supernatant from the high-speed centrifugation were loaded on SDS-PAGE and analyzed by Western blot.

Migration Assay

MDCK cells were grown in Petri dishes, induced with IPTG for 48 h, and starved for 24 h. Every Petri dish was marked, and the confluent cell monolayer was scratched along the marked line using a micropipette tip. After 30 min in the incubator, the cells were monitored by phase-contrast microscopy, with images taken at 0, 18, 24, and 48 h. The marks present in every image were aligned, and the migration distance was measured, keeping the marks as reference, in 10 different points of five fields.

Membrane Traffic

MDCK clones were induced for 48 h with 5 mM IPTG as described above. MDCK and N2A clones were rinsed in PBS and incubated at 37°C, first for 5 min with 10 μM FM4-64-FX in PBS containing 0.9 mM $CaCl_2$ and 0.5 mM $MgCl_2$ and then for 5 additional min with a new batch of the same solution containing or not 200 μM ATP for MDCK and 50 mM KCl for N2A. Cell surface labeling was removed by washing with warm PBS for 8 min. Exo- and endocytic traffic was stopped with ice-cold PBS before fixation. FM4-64 fluorescence was assayed as described by Bertrand *et al.* (2006). Coverslips were mounted and photographed as for immunofluorescence.

Time-Lapse Microscopy

MDCK clones were induced for 48 h with 5 mM IPTG and transiently transfected with actin-green fluorescent protein (GFP; a gift from Dr. Y. Goda, University College, London, United Kingdom). Coverslips were mounted in a chamber with Opti-MEM in the Deltavision RT microscope (Applied Precision, Issaquah, WA) at 37°C. LatA experiments were performed in Opti-MEM medium. Series of 12 acquisitions along the Z-axis were taken every 30 s for a total of 80 min using an Olympus 60× oil immersion objective (NA 1.42; Olympus, Hamburg, Germany) with a Coolsnap camera (Photometrics, Tucson, AZ). Data were deconvoluted and the maximum intensity projections along the Z-axis were performed with the SoftWoRx software (Applied Precision).

RESULTS

α-Synucleins Bind Actin and Affect the Properties of Its In Vitro Polymerization

The direct binding of α-synuclein and its mutant A30P to actin and the effects of the two proteins on actin polymerization were investigated by in vitro assays using highly purified preparations of the proteins (see Figure 1A for actin and wt α-synuclein; A30P α-synuclein is not shown). Both the kinetics of actin filaments assembly/disassembly and the filaments length were affected by α-synucleins. Figure 1, B and C, shows the effect of wt and A30P α-synucleins on the kinetics of actin polymerization driven by salts at low (0.1 μM) $[Ca^{2+}]$, as revealed by the increased fluorescence of pyrenylated actin. The addition of salts was followed by a ~100-s lag phase, which was not modified by α-synucleins. In contrast, the rate of polymerization, as reflected by the steep rise in fluorescence, was increased by A30P α-synuclein in a concentration-dependent manner. Interestingly, wt α-synuclein induced hardly any effect at lower concentrations and became clearly inhibitory at 11 μM, slowing the rate of polymerization and reducing the final level of polymerized actin (Figure 1C). The specificity of the effects of α-synucleins was confirmed by carrying out polymerization experiments at both low- (46 mM) and high- (116 mM) salt concentration (data not shown). The possibility of a nucleating effect of A30P α-synuclein that would accelerate the initial polymerization rate was excluded by higher resolution analyses of the initial 140 s of the slopes (inset in Figure 1B).

Actin binding/polymerization, in the presence of 11 μM wt or A30P α-synucleins, was also analyzed by ultracentrifugation and Western blotting (Figure 1D). Significant amounts of actin were recovered in the low-speed pellet (P1), which contains primarily long actin filaments and bundles, and the amount of actin recovered was increased by A30P α-synuclein. In contrast, the high-speed pellet (P2) contained a similar fraction of filamentous actin in the control and in the A30P α-synuclein samples, whereas actin recovery in this fraction was decreased by 50% in the presence of wt α-synuclein. Consistent with these results, the actin recovery in the final supernatant (fraction S), which contains mostly soluble actin, was highest in the actin/wt α-synuclein sample. Wt and A30P α-synucleins cosedimented with actin both at low and high speed. However, A30P α-synuclein was predominant in P2, whereas wt α-synuclein was predominant in S (Figure 1D). In the absence of actin, both α-synucleins were recovered in S (Figure 1D and data not shown), excluding the possibility of α-synuclein aggregation as the cause of their sedimentation. Overall, the results of Figures 1B-D demonstrate that wt α-synuclein decreases the rate and the amount of polymerized actin, and that this effect is lost by the A30P mutant, which in contrast appears to increase the rate of polymerization and to stabilize the actin filaments.

Further in vitro actin polymerization experiments with and without α-synucleins were carried out in the presence of high $[Ca^{2+}]$. Figure 1E shows that at 100 μM $[Ca^{2+}]$ the inhibition of actin polymerization by full-length wt α-synuclein was no longer appreciable, whereas the increase of actin polymerization by A30P α-synuclein, although less evident, was still observed. Thus, the divergent effects of the two α-synucleins on actin polymerization appear to be similarly modulated by Ca^{2+}.

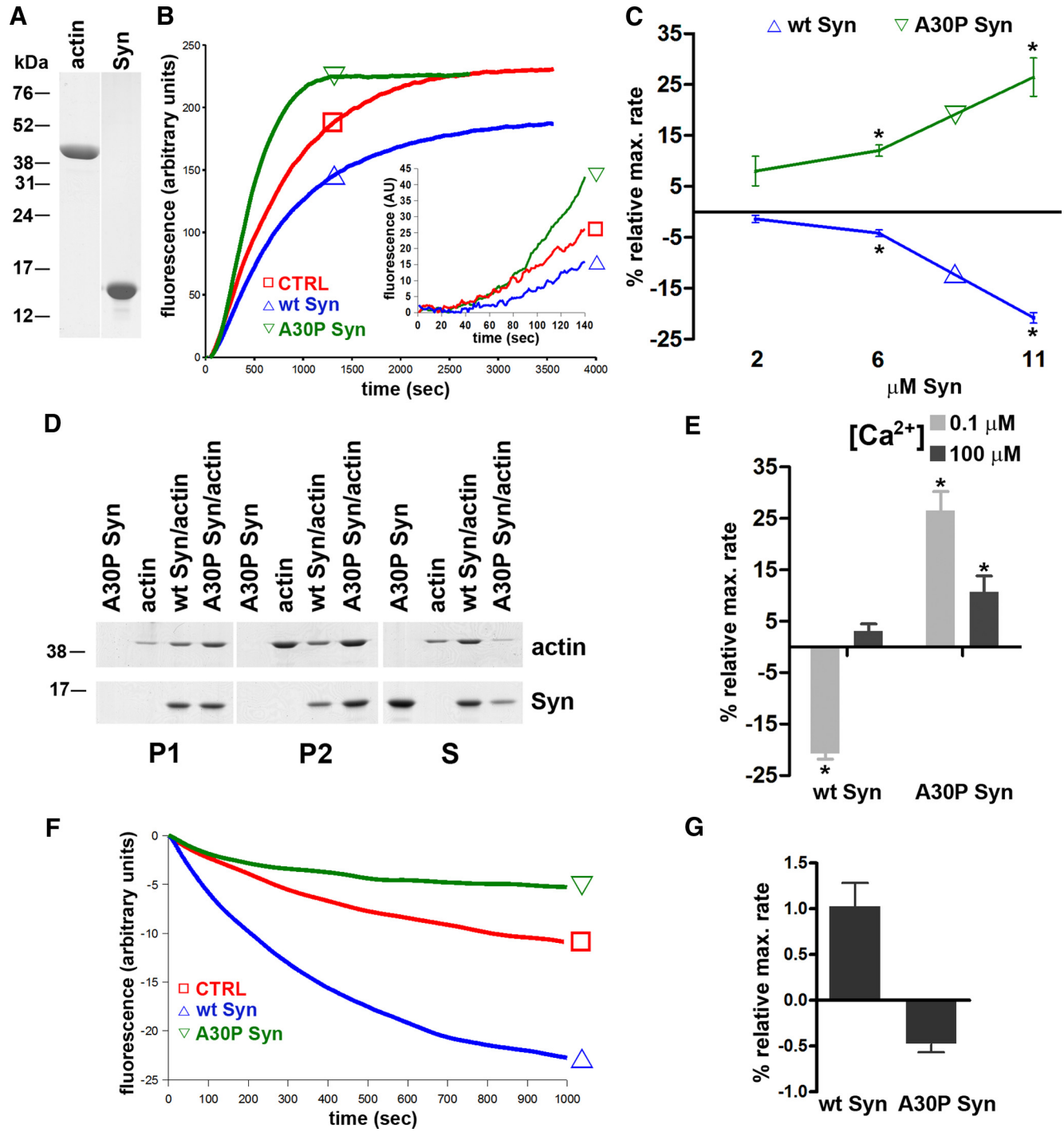

Figure 1. Effects of α-synucleins on actin polymerization/depolymerization kinetics in cell-free assays. (A) Purified actin and wt α-synuclein (5 μg) separated by SDS-PAGE and stained with Coomassie blue. (B) Kinetics of actin polymerization. Experiments were performed in a fluorometer at 30°C. Purified actin (5 μM; 5% pyrenilated) was polymerized in a solution containing 85 mM NaCl, 30 mM KCl, 1 mM $MgCl_2$, and 0.1 μM $CaCl_2$, in the absence (CTRL = controls) or presence of 11 μM wt or A30P α-synuclein. (C) Effects of various concentrations of wt or A30P α-synuclein on the actin polymerization rate at 0.1 μM $CaCl_2$. (D) Cosedimentation of wt or A30P α-synucleins (11 μM) at 0.1 μM $CaCl_2$ with actin filaments. Samples were centrifuged at 15,000 × *g* for 10 min (P1), followed by a second spin at 135,000 × *g* for 20 min (P2). S, supernatant of the P2 centrifugation (half of the supernatant was loaded). (E) Changes in the maximal rate of actin polymerization induced by wt or A30P α-synuclein (11 μM) at 0.1 or 100 μM $CaCl_2$. (F) Kinetics of actin depolymerization. Actin was polymerized in high-salt conditions as in B and subsequently diluted 10-fold in buffer without salts (see *Materials and Methods*), in the absence (CTRL) or presence of 6 μM wt or A30P α-synuclein. (G) Effects of 6 μM wt or A30P α-synuclein on the actin maximum depolymerization rate at 0.1 μM $CaCl_2$. In C, E, and G values are expressed as percentage of the control. (* $p < 0.05$).

The effect of wt α-synuclein on actin polymerization kinetics could be due to either severing of the filaments or sequestration of monomers that would slow down their incorporation into filaments. Two types of experiments were

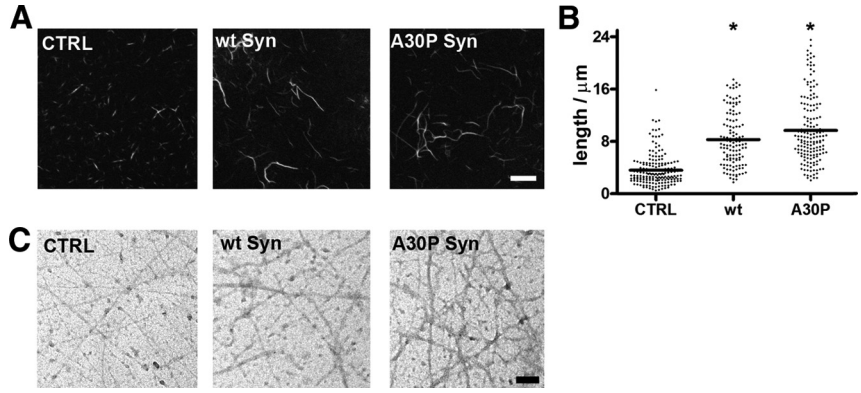

Figure 2. Effects of α-synucleins on actin filament structure. (A) Fluorescence microscopy analysis of actin filaments generated by a 30-min incubation at 30°C of 5 μM actin in a solution containing 85 mM NaCl, 30 mM KCl, 1 mM $MgCl_2$, and 0.1 μM $CaCl_2$, in the absence (CTRL) or presence of 11 μM wt or A30P α-synuclein. Actin filaments were visualized by labeling with FITC-phalloidin. (B) Length distribution of the filaments shown in A. For each condition, 130–170 bundles from five fields of view were analyzed. Horizontal bars indicate mean values (* $p < 0.05$). (C) Negative staining of actin bundles prepared as in A. Bar, (A) 5 μm; (C) 0.1 μm.

performed to answer this question. We investigated the effect of α-synucleins on depolymerization driven by dilution of prepolymerized actin in a buffer without salts. Figure 1, F and G, show that, compared with the control, wt α-synuclein induced a 100% increase of the rate of depolymerization. On the contrary, A30P α-synuclein decreased the depolymerization rate by 50%, indicating a stabilization of actin filaments. However, when actin was diluted to levels below the critical concentration, neither wt nor A30P α-synuclein had any effect on the rate of depolymerization (Supplementary Figure S1, A and B). In sedimentation experiments, no increase in soluble actin was detected when either α-synuclein was added to prepolymerized actin in either the presence or absence of the capping agent cytochalasin D (Supplementary Figure S1C). Both results exclude a severing effect of wt α-synuclein and confirm its effect to be due to monomer sequestration.

The structure of polymerized actin filaments was analyzed at the light and electron microscope level (Figure 2). The filaments polymerized in the presence of either α-synuclein and labeled with fluorescent phalloidin appeared thicker and longer than the control filaments. α-Synuclein increased the average filament length by 35%, and A30P α-synuclein by 60% (Figure 2, A and B). Electron microscopy of negatively stained samples revealed that the filaments assembled in the presence of either wt or A30P α-synuclein consisted of thin bundles composed by few fibrils, whereas virtually no bundles were observed in the control samples (Figure 2C). These results indicate a qualitatively similar bundling activity of the two α-synucleins, which however have opposite effects on the kinetics of actin polymerization.

A30P α-Synuclein Induces Cytoskeleton Disruption in N2A Cells

The murine neuroblastoma N2A cell line was chosen for the cellular investigation of the interactions between α-synucleins and the actin cytoskeleton. N2A cells express very low levels of endogenous α-synuclein, hardly appreciable by either Western blotting or immunocytochemistry (Figure 3, A–D). In these cells, concentrations of α-synucleins comparable to those existing in the brain (Shibayama-Imazu *et al.*, 1993; Nakajo *et al.*, 1996) were reached by either delivery of recombinant wt or A30P α-synucleins or transfection of the corresponding cDNAs. The concentration of exogenous α-synucleins in the cells loaded by SLO permeabilization (Walev *et al.*, 2001) followed by Ca^{2+}-dependent membrane resealing was ~5 μM, as revealed by Western blotting (Figure 3A). In both control and wt α-synuclein–loaded cells (Figure 3B, CTRL and wt Syn), as well as in nonpermeabilized N2A cells, fluorescent phalloidin revealed a predominant distribution of F-actin in the regular crown of stress fibers beneath the plasma membrane (Figure 3D, CTRL). In contrast, in the cells loaded with A30P α-synuclein the cytoskeleton appeared disrupted, with retraction of the stress fibers to the perinuclear area and ensuing reduction of the cell size (Figure 3B, A30P Syn).

Further studies in stable clones of N2A expressing ~6 μM levels of wt or A30P α-synuclein (Figure 3C) revealed a cytoskeleton morphology similar to that of cells loaded with the α-synucleins by SLO (Figure 3B). Control cells and cells expressing wt α-synuclein exhibited the crown of stress fibers beneath the plasma membrane (Figure 3D, CTRL and wt Syn), whereas cells expressing A30P α-synuclein displayed retraction of the actin cytoskeleton and apparent reduction of the cell size (Figure 3D, A30P Syn). N2A clones expressing α-synucleins showed a growth rate similar to that of nontransfected N2A cells (Supplementary Figure S2A) and no increase of caspase-3 activity (not shown), suggesting a tendency to apoptosis comparable to that of control cells.

A30P α-Synuclein Induces the Formation of Actin-enriched Foci during Dynamic Cytoskeletal Remodeling

To analyze the effect of α-synucleins on the assembly of new actin filaments in living cells, N2A stable clones expressing α-synucleins were exposed for 5 min to LatA, a drug that induces depolymerization of actin filaments by sequestering actin monomers (Spector *et al.*, 1999). After treatment, the drug was washed out and the cells were reincubated in conventional medium to let their cytoskeleton repolymerize. Figure 4A shows filamentous and soluble fractions of actin separated by high-speed centrifugation, in either the absence or presence of LatA. At steady state ~80% of the total actin was polymerized, whereas after 5 min of LatA, ~70% was soluble. Immunofluorescence of cells fixed and analyzed at various time points during LatA experiments (Figure 4B) revealed a clear disruption of the actin cytoskeleton in the cells treated with the drug. The cytoskeleton disruption was slightly more pronounced in the wt α-synuclein–expressing cells. Wash out of the drug was followed by reorganization of the cytoskeleton, which however was still incomplete after 20 min. In the A30P Syn-expressing cells, the cytoskeleton, already disrupted at rest, during recovery from LatA exhibited a number of discrete, subplasmalemma puncta, composed by a core of A30P synuclein surrounded by a shell of compacted actin (defined from hereon as actin-rich foci). Thus, in these samples, actin was distributed both in the subplasmalemma crown of fibers, and in the small actin/A30P-rich foci (Figure 4B, bottom row). The reduction of cell

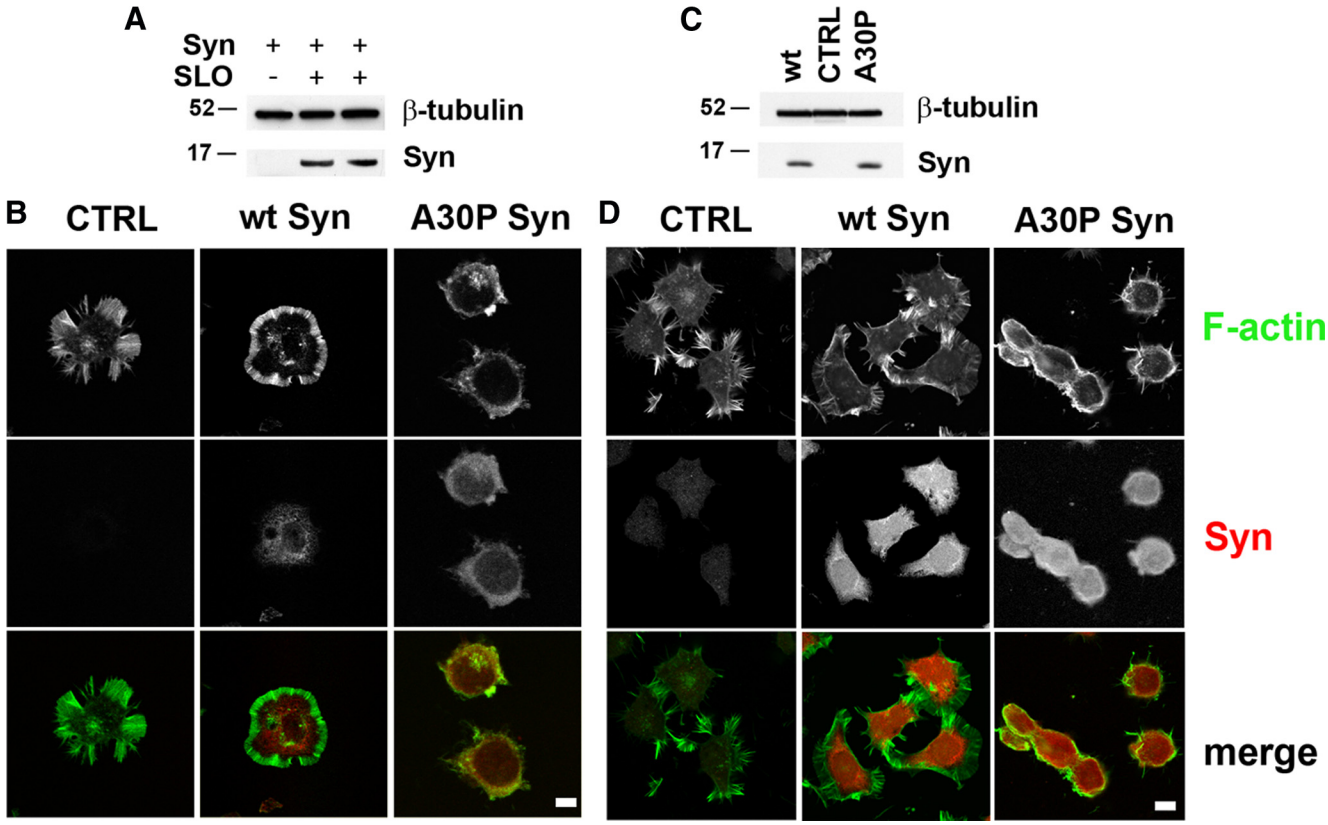

Figure 3. A30P α-synuclein disrupts the actin cytoskeleton of N2A neuroblastoma cells. (A) Western blot of α-synuclein internalization in N2A cells incubated with 12 μM recombinant α-synuclein in control conditions or after permeabilization with SLO. (B) Distribution of actin and α-synucleins in SLO-permeabilized cells either unloaded (CTRL) or loaded with 12 μM wt or A30P α-synucleins. (C) Western blot analysis of α-synucleins expression in nontransfected (CTRL) or stably transfected N2A cells. (D) Distribution of actin and α-synucleins in nontransfected (CTRL) or stably transfected N2A cells. (A) and (C) β-tubulin is shown as an internal standard. (B and D) Actin was visualized by FITC-labeled phalloidin (green) and α-synuclein by indirect immunofluorescence (red). Notice the disappearance of the peripheral actin spikes with retraction of actin to the perinuclear area in the cells loaded (B) or transfected (D) with A30P α-synuclein, but not in those loaded or transfected with wt α-synuclein. Bars, 10 μm.

size, that was already noticed at steady state in the A30P cells (see also Figure 3, B and D), was even more pronounced upon disassembly of the actin cytoskeleton and during the first phases of reassembly (Figure 4C).

A30P α-Synuclein Induces Cytoskeletal Modification Also in Epithelial MDCK Clones

To investigate the effects of the A30P α-synuclein–dependent disruption of actin cytoskeleton on motility processes (such as wound healing and migration) that cannot be investigated in N2A cells, we turned to canine MDCK epithelial cells. This line, which lacks endogenous α-synuclein, grows in tight monolayers and is characterized by a well-defined network of actin fibers running below the plasma membrane (Yamazaki *et al.*, 2007). Inducible MDCK clones were generated, which express moderate levels (~2 μM) of either wt or A30P α-synuclein upon 48-h incubation with 5 mM IPTG (Figure 5A). Also in this case, the expression of α-synucleins appeared to induce no increased frequency of apoptosis (not shown).

In MDCK cells most actin was assembled, and ~70% became disassembled after 10 min of LatA treatment (Figure 5B). When control and α-synuclein–expressing MDCK cells were analyzed by phalloidin labeling, no significant differences in the cytoskeletal organization were revealed under resting conditions (Figure 5C). This result, however, did not exclude an effect of α-synucleins on actin undergoing dynamic rearrangement. MDCK monolayers were therefore fixed at various time points after exposure to LatA and recovery. In control MDCK cells, LatA induced a disruption of the actin network into fragments scattered throughout the cytoplasm, and a partial release of the cell-to-cell contacts that were complete after 10-min treatment. The formation of new actin fibers, appreciable already at ~20-min recovery after LatA washout, was virtually complete after ~40 min with the reestablishment of both the ordered subplasmalemma network and the intercellular contacts (Supplementary Figure S2B and Figure 5C). Treatment of control MDCK cells with IPTG did not modify the time course of actin filament disassembly and reassembly (Supplementary Figure S2B). In MDCK cells induced with IPTG for wt α-synuclein expression (Figure 5C), the disassembly of filaments was much faster. In fact, the disruption of the actin cytoskeleton visible after 3-min treatment with LatA was similar to that seen in control cells after 10 min. Furthermore, the recovery of the cytoskeleton was much slower: no actin filaments were reformed after 20 min, and after 60 min many short fragments of actin were still scattered and the cell-to-cell contacts were incompletely reestablished. In cells expressing A30P α-synuclein the alterations of the actin cytoskeleton appeared even more profound. Filamentous actin structures formed during the first 3 min of incubation with LatA were

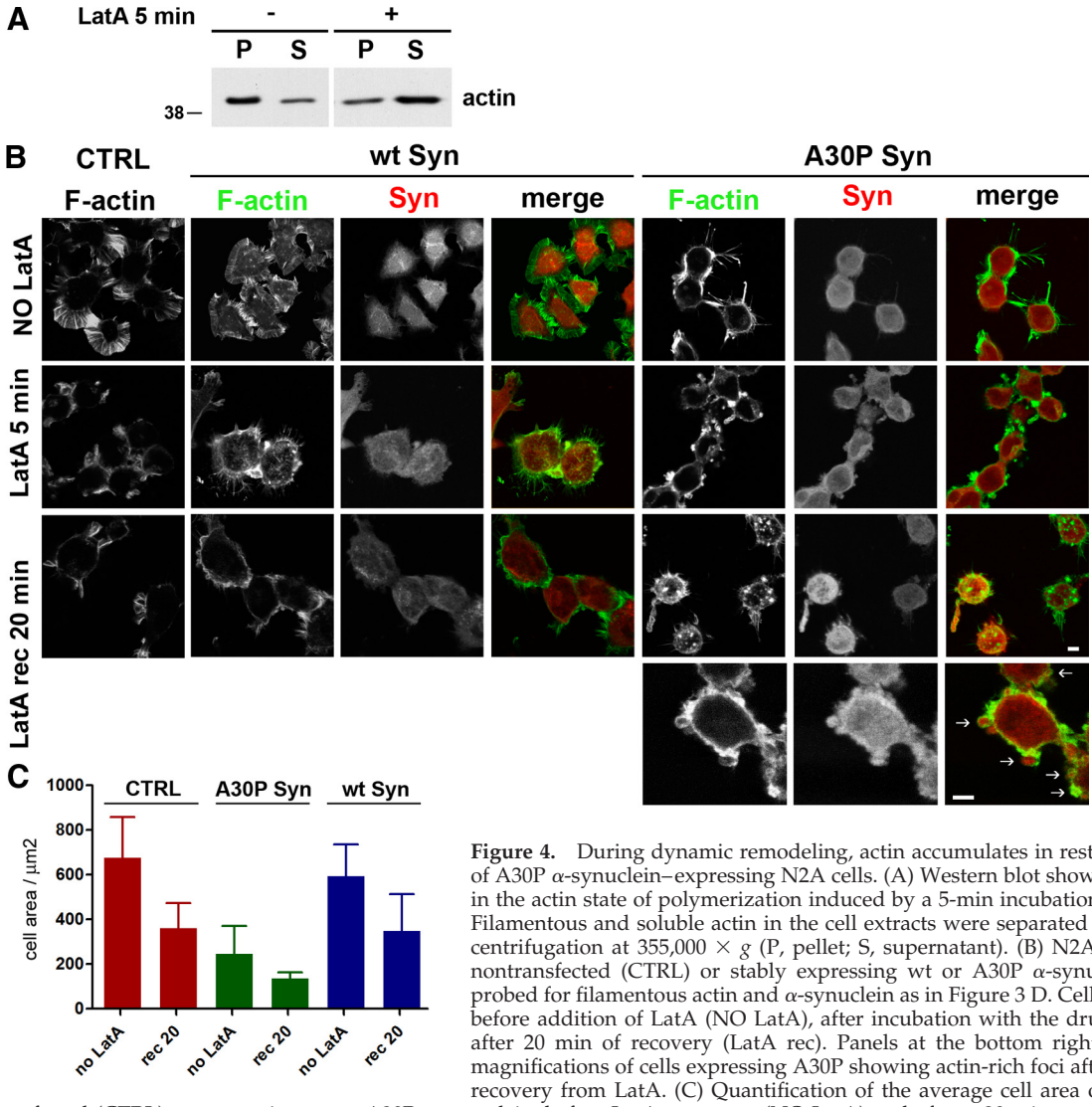

Figure 4. During dynamic remodeling, actin accumulates in restricted zones of A30P α-synuclein–expressing N2A cells. (A) Western blot showing changes in the actin state of polymerization induced by a 5-min incubation with LatA. Filamentous and soluble actin in the cell extracts were separated by a 30 min centrifugation at 355,000 × *g* (P, pellet; S, supernatant). (B) N2A cells either nontransfected (CTRL) or stably expressing wt or A30P α-synucleins were probed for filamentous actin and α-synuclein as in Figure 3 D. Cells were fixed before addition of LatA (NO LatA), after incubation with the drug (LatA) or after 20 min of recovery (LatA rec). Panels at the bottom right are higher magnifications of cells expressing A30P showing actin-rich foci after 20 min of recovery from LatA. (C) Quantification of the average cell area of N2A cells either nontransfected (CTRL) or expressing wt or A30P α-synuclein, before LatA treatment (NO LatA) and after a 20 min recovery from a 5-min exposure to the drug (rec 20). Bars, 10 μm.

no longer evident after 10 min, when the actin cytoskeleton was completely disassembled. During recovery, however, actin was distributed in foci including A30P α-synuclein that were very prominent at 20 min and remained evident up to 40 min. When analyzed in 3D, these foci appeared distributed close to the plasma membrane, more often near the cell-to-cell contacts and rarely below the apical and basolateral surfaces (Figure 5D). These structures were transient, because after 60 min of recovery A30P α-synuclein–expressing cells exhibited an ordered actin network, similar to that of control cells (Figure 5C, 60-min row). The presence of the foci was quantified by measuring the areas exhibiting actin fluorescence intensity above an arbitrary threshold (Figure 5E). Of note, at 20-min recovery, the area of A30P α-synuclein cells with high fluorescence intensity was 65% higher than in control and wt α-synuclein cells.

In principle, the effects of α-synuclein on actin dynamics could depend on phosphorylation events mediated by interactions of the protein with kinases or phosphatases. However, this did not appear to be the case, because the levels of actin phosphorylation were similarly low in all MDCK clones (Supplementary Figure S2C).

A30P α-Synuclein Shows Increased Interaction with Filamentous Actin and No Binding to Soluble Actin

Subcellular fractions were isolated from MDCK clones exposed to LatA for 10 min, followed by a 20-min recovery. Consistent with the results of the fluorescence experiments, a higher amount of F-actin sedimented together with the mutated α-synuclein in the high-speed pellet, whereas more soluble actin was recovered in the supernatant prepared from the cells expressing wt α-synuclein (Figure 6A).

The interaction of α-synucleins with actin at steady state and in the course of repolymerization was investigated also by α-synuclein IP from MDCK extracts. A higher fraction of actin co-IP with α-synuclein was observed at rest in wt α-synuclein–expressing cells and at 20-min recovery in A30P α-synuclein–expressing cells (Figure 6B).

Similar co-IP experiments were carried out before and at the end of the LatA treatment, using the final supernatant (i.e., the fraction containing soluble actin isolated by ultracentrifugation) as the starting material. We found that the anti-α-synuclein antibody was able to coimmunoprecipitate soluble actin only from the supernatants of wt α-synuclein

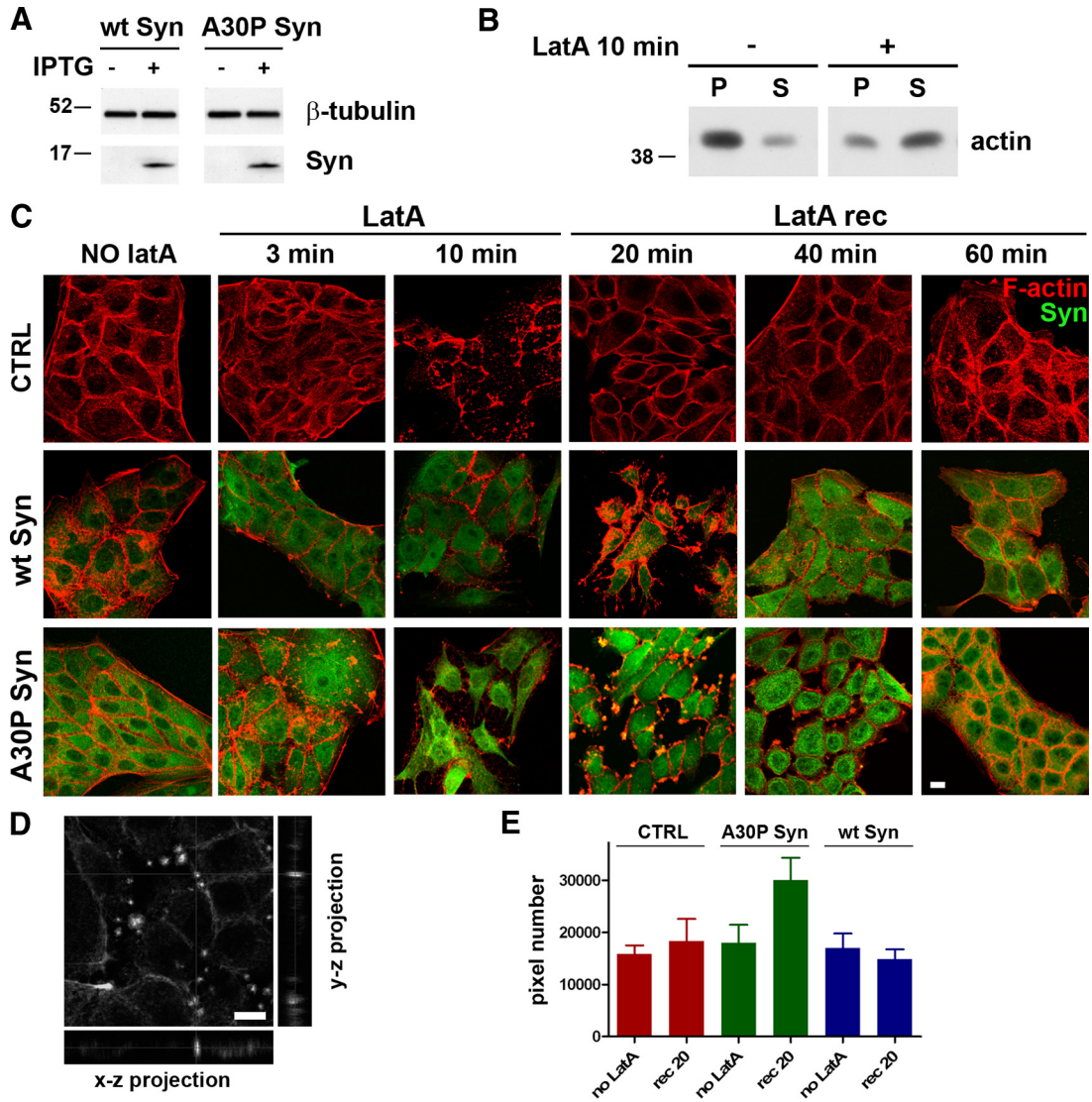

Figure 5. During actin repolymerization A30P α-synuclein induces the formation of transient actin-rich foci in MDCK cells. (A) Expression of wt or A30P α-synucleins in IPTG-induced clones of MDCK cells. β-Tubulin is shown as an internal standard. (B) Actin distribution in the pellet and supernatant fractions of extracts of MDCK cells treated or not with LatA as in Figure 4A. (C) Actin repolymerization assays. MDCK cells expressing wt or A30P α-synucleins were fixed and probed for F-actin (red) and α-synuclein (green). Cells were fixed before addition of LatA (NO LatA), after 3- and 10-min incubation with the drug (LatA), and after 20, 40, and 60 min of recovery from a 10-min incubation (LatA rec). (D) Middle section of a 3D stack of images on the Z axis showing actin-rich foci in A30P α-synuclein–expressing cells after 20 min of recovery. Right and bottom panels, the Y-Z and X-Z projections at positions marked by the vertical and horizontal gray lines, respectively. (E) Quantification of the cell areas exhibiting actin fluorescence above an arbitrary threshold value in the images of MDCK cells either not induced (CTRL) or expressing wt or A30P α-synucleins. Measurements were performed in cells fixed before LatA addition or at 20-min recovery. A total of 400 × 400 pixels were analyzed in 20 fields of view in five different experiments. The graph highlights the presence of areas of actin compaction in A30P cells at the 20-min recovery time. Bars, 10 μm.

and not of A30P α-synuclein–expressing cells (Figure 6C). Taken together with the previous observations made with in vitro assays (Figure 1 and Supplementary Figure S1) and in intact cells (Figures 4 and 5), these results confirm that the actin depolymerization induced by wt α-synuclein is due to monomer sequestration, which is an activity lost by the A30P mutant (Figure 6D).

A30P α-Synuclein Inhibits the Generation of Lamellipodia and Filopodia during Actin Remodeling

The time course of the changes in actin distribution during LatA experiments was investigated also by time-lapse videomicroscopy, using MDCK clones, control and expressing wt or A30P α-synucleins, transiently transfected with an actin-GFP chimera (Supplementary Videos 1–3 and frame sequences in Figure 7A). During LatA recovery, control cells (Supplementary Video 1 and top row of Figure 7A) were seen to emit actin-rich protrusions and filopodia, already visible at 2 min after LatA washout and exhibiting the shape of lamellipodia from 20 min onward. These changes in shape were accompanied by movement of the cell. Wt synuclein–expressing cells (Supplementary Video 2 and middle row of Figure 7A) exhibited similar changes; however, the reassembly of filaments was slower, and stress fibers reappeared

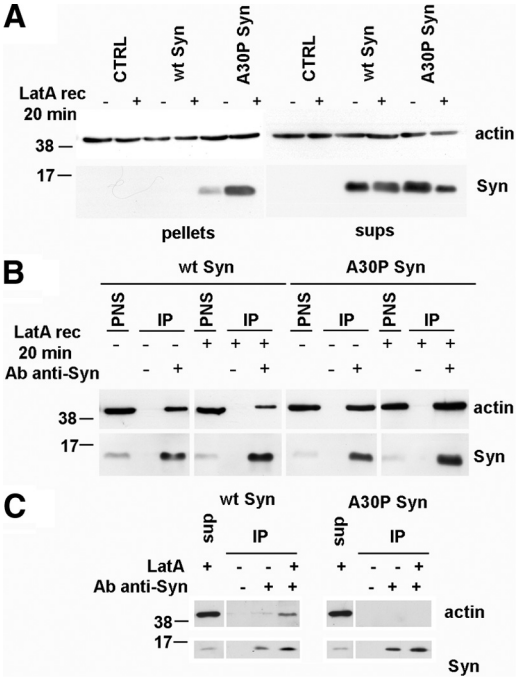

Figure 6. Co-IP of actin and wt or A30P α-synuclein from homogenates of MDCK cells expressing wt or A30P α-synucleins. (A) Stably transfected MDCK cells, CTRL, and those expressing wt or A30P α-synuclein were lysed under control conditions or after a 20-min recovery from a 10-min incubation with LatA. After a 30 min centrifugation at 355,000 × *g*, proteins from the pellets and the final supernatants (sups) were stained with anti-α-synuclein and anti-actin antibodies. At 20-min recovery (LatA rec 20 min), F-actin is increased in the A30P α-synuclein–expressing cells, whereas soluble actin is more abundant in the wt α-synuclein–expressing cells. (B) PNS from MDCK cells expressing wt or A30P-α-synuclein treated as in A were subjected to IP with the anti-α-synuclein antibody. In the case of wt α-synuclein the coprecipitated actin was slightly more abundant in the untreated sample, whereas in the case of A30P α-synuclein it was more abundant after LatA recovery. The amount of PNS loaded corresponds to 5% of the total cell extracts. (C) Final supernatant obtained as in A from MDCK cells under control conditions or after 10-min incubation with LatA were subjected to IP as in B. No coprecipitation of soluble actin with A30P α-synuclein was observed, whereas wt α-synuclein coimmunoprecipitated soluble actin especially when its amount was increased by LatA-induced depolymerization.

only after a 1-h recovery (Figure 7A). In contrast, the A30P α-synuclein cells (Supplementary Video 3 and bottom row of Figure 7A) were almost immobile, possibly because of the delayed repolymerization of organized actin filaments. Their intracellular actin-rich foci, already visible during the first minute of recovery, increased in size and number thereafter, becoming quite evident between 10 and 20 min, exhibiting continuous random movements, and pushing out and rolling beneath the cell surface. The subsequent disappearance of these structures was slower than in the fixed samples (Figure 5C), with a few foci still detectable at 60 min.

Figure 7B shows the values of the cell area at different times during LatA incubation and washout. In the control sample the values were high, because of the formation of lamellipodia; the area of A30P α-synuclein cells was smaller and increased only slightly during the whole LatA recovery period. Figure 7C illustrates the cells mobility, assayed by taking the center of the nucleus as a reference point. The movement, low at steady state when the cells were part of the monolayer, increased during LatA recovery. Wt α-synuclein cells showed a rate similar to that of control cells, whereas A30P α-synuclein cells were less mobile with a rate of movement 50% lower than control cells from 20 min of recovery on.

Wt α-Synuclein Accelerates, and A30P α-Synuclein Slows Down the MDCK Cell Migration

The effect on actin organization that is induced by expression of α-synucleins in MDCK clones prompted us to investigate cell migration. Inducible MDCK cells were cultured for 48 h with or without IPTG, up to complete confluence. Monolayers were then scratched along single lines with a micropipette tip, and the distance covered by the cells in the scratched space was measured at various time points. Migration of the wt α-synuclein cells was faster and that of the A30P α-synuclein cells was slower than migration of control cells. At 48 h, the wt α-synuclein cells had migrated an ~2.2-fold longer distance than control cells, whereas the A30P α-synuclein cells only about one-third that of control cells (Figure 8).

Surface Traffic of Membranes in MDCK and N2A Clones Is Differentially Affected by wt and A30P α-Synuclein

Membrane traffic to the apical plasma membrane was investigated in monolayers of inducible MDCK clones, which were first exposed to the membrane fixable version of the FM4-64 dye (Angleson and Betz, 1997) and then incubated for 5 min with or without 0.2 mM ATP, a treatment known to stimulate exo- and endocytosis from the apical surface of the cell via increase of $[Ca^{2+}]_i$ (Llorente *et al.,* 2000). After washing to remove the noninternalized dye, the cells were fixed and then analyzed at the confocal microscope. As shown in Figures 9, A and B, the FM4-64 fluorescence of nonstimulated control, wt, and A30P α-synuclein cell monolayers were similar, suggesting that constitutive exo- and endocytosis was taking place at similar rates. ATP stimulation induced a more than 40% increase of fluorescence in both controls and wt α-synuclein–expressing cells, whereas in the A30P α-synuclein–expressing cells fluorescence remained unchanged (Figure 9B). Similar experiments were carried out in neuronal-like N2A cells stably expressing α-synucleins, stimulated for 5 min by depolarization with high K^+. In control cells and in those expressing wt α-synuclein stimulation induced a 100% increase in fluorescence, indicating a large increase of exo- and endocytosis. In the A30P α-synuclein cells the fluorescence, which was ~50% higher than in control cells at rest, exhibited only a small increase upon stimulation (Figure 9C).

Wt α-Synuclein Increases Actin Instability and A30P α-Synuclein Induces Actin Foci in Hippocampal Neurons

To establish whether the results obtained with wt and A30P α-synucleins were representative also of the activities of the proteins in neurons, experiments were carried out in embryonal hippocampal neurons isolated from the commercial C57BL/6S mouse carrying an α-synuclein gene deletion. In agreement with the data on α-synuclein knockout mice (Abeliovich *et al.,* 2000; Cabin *et al.,* 2002), these animals appeared phenotypically normal.

The actin cytoskeleton of hippocampal neurons from wt C57BL/6J mice and of electroporated hippocampal neurons from C57BL/6S mice expressing or not wt or A30P α-synuclein were found to be very similar (Figure 10A). At rest, (Figure 10A, NO LatA) wt and A30P α-synucleins appeared distributed in the cytosol of neuronal cell bodies and

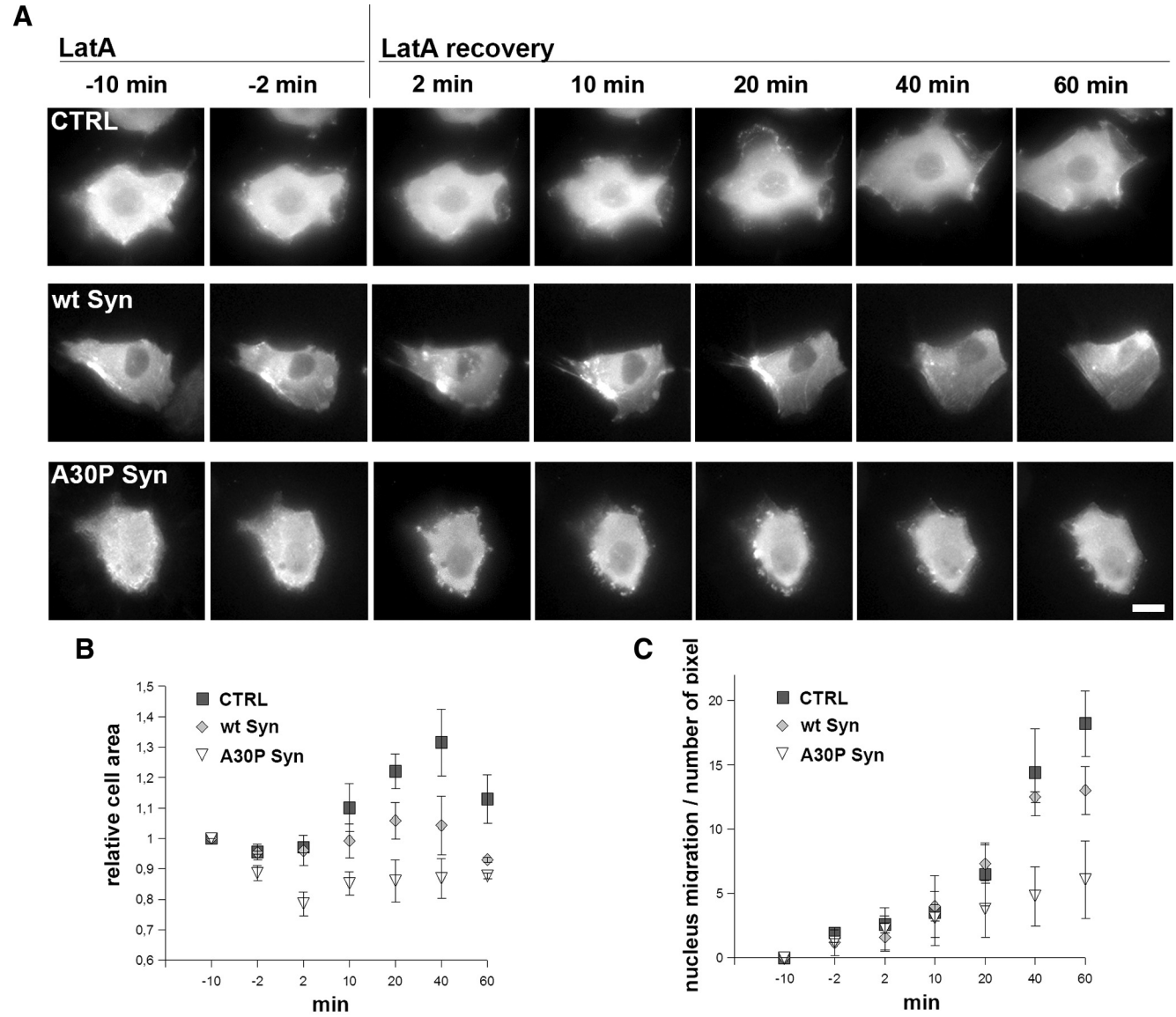

Figure 7. Time-lapse microscopy of MDCK cells during LatA treatment and washout. A30P α-synuclein expression inhibits actin reorganization, lamellipodia formation and cell movement. (A) The three rows show frames from time-lapse microscopy videos (Videos 1–3) of CTRL, wt α-synuclein, or A30P α-synuclein–expressing MDCK cell transfected with actin-GFP, during LatA treatment and washout. Notice in the top row the appearance of lamellipodia guiding the cell movement during wash out of LatA; in the low bottom row the appearance, already at 2 min, of large subplasmalemma GFP-actin aggregates persisting up to the end of the experiment. (B) Relative changes of the average cells area in MDCK cells during LatA incubation and recovery as in A. The area is normalized to the −10-min time point. (C) Changes of the rate of cell movement in MDCK during LatA incubation and recovery as in A, expressed as the traveled distance of the nucleus. The points in B and C are averages (±SEM) of three different measurements from independent experiments. Bar, 10 μm.

often were localized in fine, densely labeled structures in the proximal regions of neurites and all along the processes, with faint diffused labeling at growth cones (Kahle *et al.*, 2000; Lesuisse and Martin, 2002; Quilty *et al.*, 2003). Compared with control neurons, the major neurite of A30P α-synuclein neurons was significantly shorter, whereas wt α-synuclein neurons showed a more prominent elongation of the average minor neurites (Figure 10C).

To study the effect of α-synucleins on actin remodeling, hippocampal neurons were incubated in conditioned medium for 1 h at 37°C with 1 μM LatA, and the recovery of their cytoskeleton was investigated for up to 2 h after washout of the drug. In LatA-treated neurons, the fluorescent phalloidin staining was strongly decreased, and filamentous actin appeared fragmented, scattered in spots in the cell bodies and along neurites (Figure 10A, LatA). In control and wt α-synuclein neurons a loss of filamentous actin staining was evident at the tips of the neurites, where actin remodeling is more active and more sensitive to the action of LatA (Bradke and Dotti, 1999). On the contrary, the A30P α-synuclein neurons treated with LatA exhibited filamentous actin concentrated in small foci, particularly visible along the neuritic processes at their proximal regions, where A30P α-synuclein was also enriched.

Cytoskeleton recovery was analyzed at 1 and 2 h after LatA washout. After a 1-h recovery from LatA the cell area of control neurons appeared increased because of newly formed lamellipodia-like structures. At 2-h recovery, new

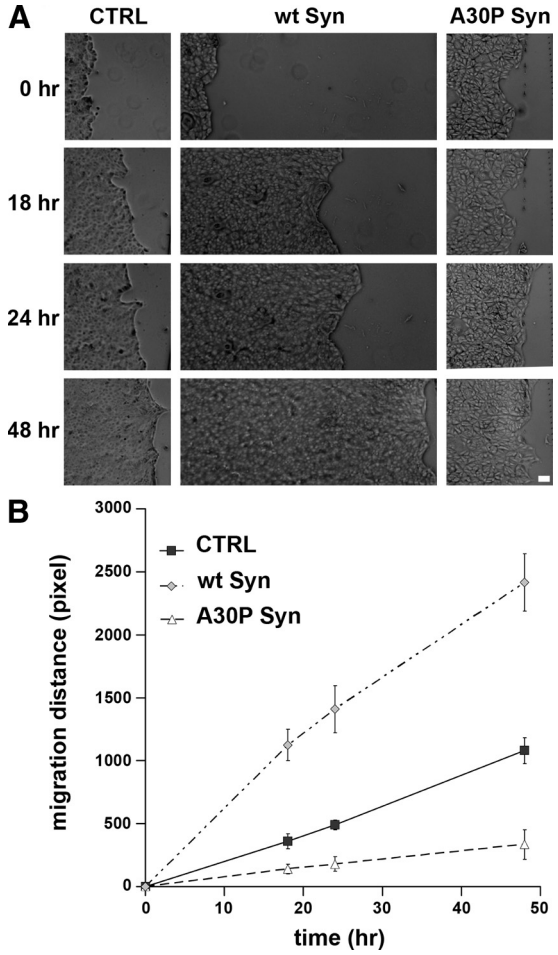

Figure 8. Wt and A30P α-synucleins have different effects on cell migration into scratch wounds. (A) Monolayers of MDCK cells, CTRL and those expressing wt or A30P α-synucleins, were cultured until confluence and then scratched with a micropipette tip. Phase-contrast images were collected at different time points after scratching as indicated. (B) The graph shows the migration of MDCK cells as such as those illustrated in A. Each point is the average ± SD of 10 different measurements in five microscopic fields. Bar, (A) 500 μm.

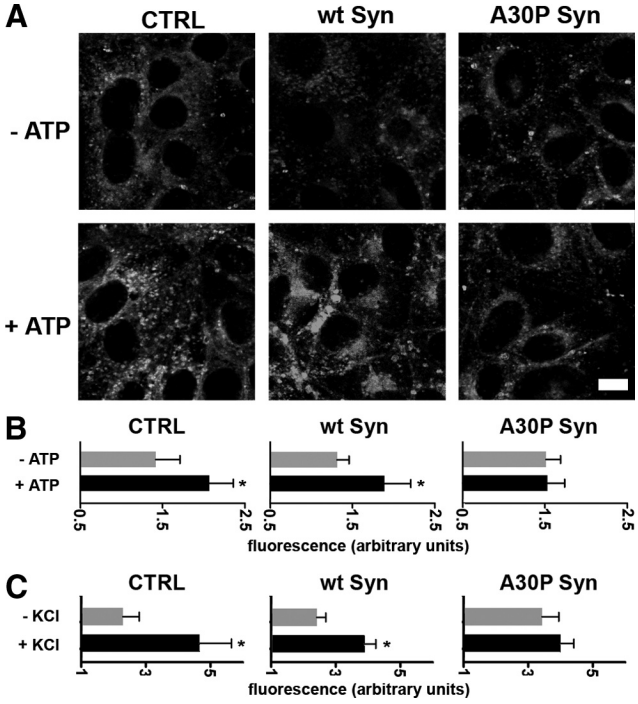

Figure 9. A30P α-synuclein affects exo- and endocytosis. (A) CTRL, wt, or A30P α-synuclein–expressing MDCK cells were incubated with FM4-64-FX for 5 min, followed by an additional 5-min incubation with the dye in the presence or absence of 200 μM ATP. After washing to eliminate the noninternalized dye the cells were fixed and analyzed for FM fluorescence. Bar, 10 μm. (B) Quantification of total fluorescence from five different fields of two independent experiments. Notice the lack of ATP-induced exo- and endocytosis increase in A30P α-synuclein–expressing cells. (C) Experiment similar to that described in A performed on N2A cells loaded with FM 4-64-FX and either nonstimulated or depolarized with 50 mM KCl. Notice the decreased K^+-induced exo- and endocytic response in A30P α-synuclein–expressing cells. (B and C) Fluorescence values of are expressed as arbitrary units ± SD; * $p < 0.05$.

neurites were growing, and actin filaments reformed along their shafts and at their terminals. In wt α-synuclein neurons, actin instability was more profound, with the formation of more abundant lamellipodia-like structures, thus resulting in a significant increase of the cell body area (Figure 10, A, LatA rec 1 h, B, asterisks, and D). At 2-h recovery, wt α-synuclein neurons still showed a significant increase in the cell body area, whereas the body area of control neurons had returned to the steady-state values (Figure 10, A, LatA rec 2 h, and D). Apart from a faint diffused labeling at the growth cones, filamentous actin staining was still less intense in wt α-synuclein than in control neurons, suggesting a delay in actin repolymerization and in the reconstitution of the actin network.

In A30P α-synuclein neurons, the cytoskeleton was differently affected during recovery. After 1 h, actin, intensely stained by phalloidin, was still concentrated in the foci, was rich of A30P α-synuclein, and was distributed all along the neurites (Figure 10, A, LatA rec 1 h, B, arrowheads, and E). Final recovery of the cytoskeleton morphology of A30P α-synuclein-neurons, with actin filaments along the neurites and enriched at the levels of their terminals, was reached only after 2 h from LatA washout as in the control neurons. The interaction between endogenous α-synuclein and actin also was investigated in the brain tissue. Figure 10F shows that α-synuclein, isolated by high-speed centrifugation from the final supernatant of adult rat brain homogenates, is coimmunoprecipitated by the anti-actin antibody.

DISCUSSION

On the basis of a combination of experiments, in vitro assays, and in vivo studies in three types of cells chosen on the basis of their differentially favorable properties, we have identified modulation of actin dynamics as a novel function of wt α-synuclein. In addition, we have found that this function is greatly altered when α-synuclein includes A30P, a mutation associated with autosomal dominant forms of PD. In all our experiments, the concentrations of α-synucleins used were analogous to the average levels of the protein in the brain (Shibayama-Imazu *et al.*, 1993; Nakajo *et al.*, 1996) and lower than those existing in at least some synapses (Fortin *et al.*, 2005; Tao-Cheng, 2006). Our results therefore cannot depend on excess of the protein, rather, they demonstrate that the α-synuclein/actin interaction can have an

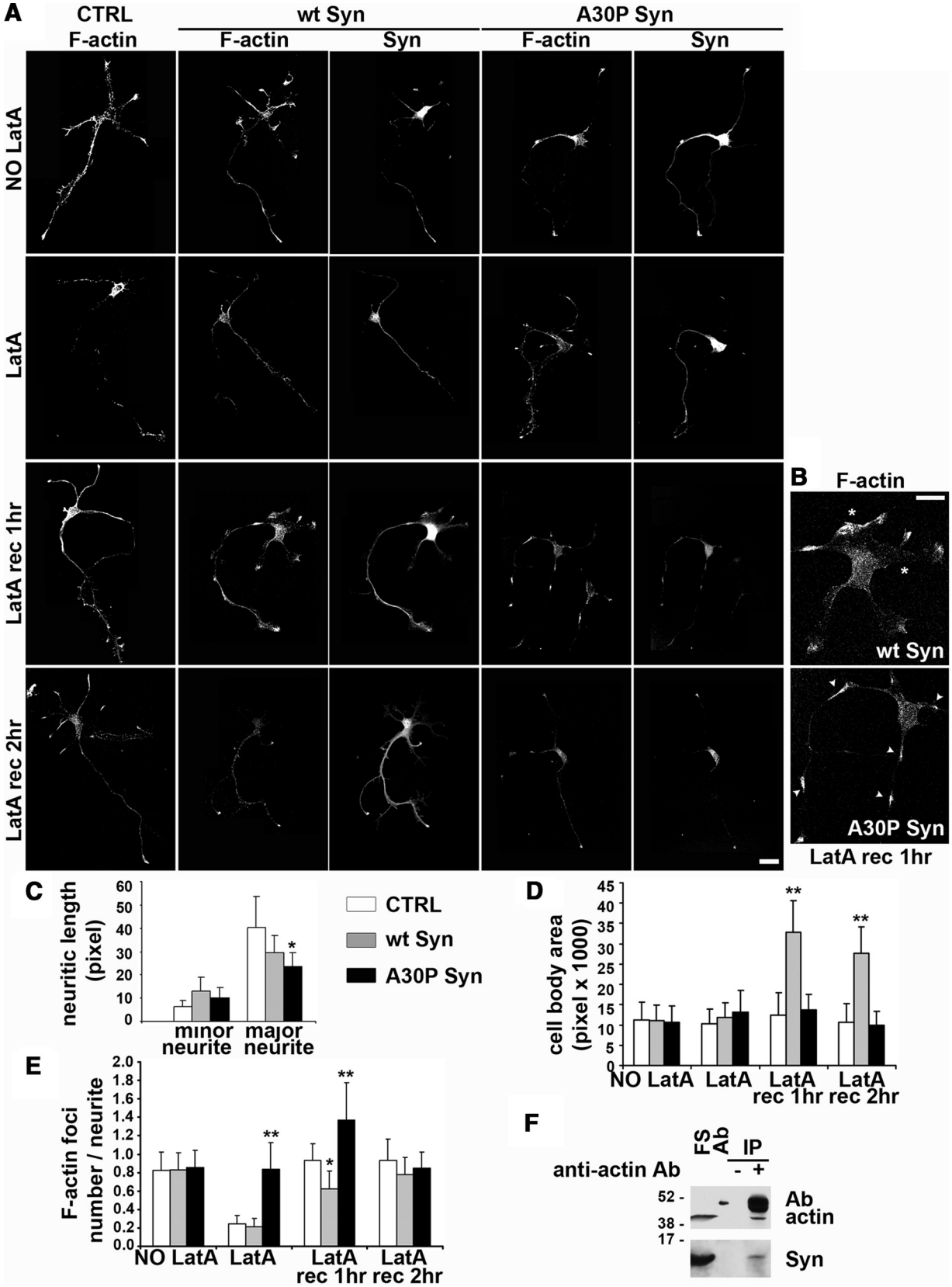

Figure 10. Wt α-synuclein increases actin instability and A30P α-synuclein induces the formation of actin foci in hippocampal neurons. (A) Immunofluorescence analysis of embryonic hippocampal neurons electroporated either with an empty vector (CTRL) or with the constructs coding for wt or A30P α-synuclein. Neurons were fixed and probed for filamentous actin and α-synucleins at 2DIV, either under control conditions or after a 1-h LatA incubation, followed or not by recovery (LatA rec) for the indicated time points. (B) Higher magnification of the area

important role in both the physiology and the pathology of the brain.

In the cell-free experiments with $[Ca^{2+}]$ as low as the cytosolic $[Ca^{2+}]$ of resting neurons, wt α-synuclein was found to induce a slowing down of polymerization and an acceleration of depolymerization, two effects most likely due to a sequestration of actin monomers. When $[Ca^{2+}]_i$ was raised to levels analogous to those of depolarized neurons, the slowing down of actin polymerization was greatly reduced. This effect, possibly occurring through the C-terminal domain of the protein that includes a low affinity Ca^{2+}-binding site (Nielsen *et al.,* 2001), might contribute to the increased plasticity of the cytoskeleton at stimulated synapses.

The actin monomer sequestration by wt α-synuclein, which we hypothesized based on the in vitro results, was strongly reinforced by results in intact cells (two cell lines, N2A and MDCK, and primary cultures of embryonal hippocampal neurons) and by results of co-IP with subcellular fractions derived from MDCK cells. In both these series of experiments a critical tool was LatA, the well-known actin monomer sequestering drug. LatA was used to analyze separately, within the cell, the local depolymerization of actin, taking place by its action, from the repolymerization taking place after drug washout. The latter process resembles the in vitro de novo actin polymerization. In agreement with the actin sequestration hypothesis, the depolymerization and the repolymerization observed in the cells expressing wt α-synuclein were qualitatively similar to those of control cells except for their faster and slower rates, respectively.

The importance of wt α-synuclein in the regulation of actin dynamics was confirmed by experiments of cell physiology. Migration of MDCK cells transfected with wt α-synuclein, a classical cytoskeleton-dependent function (Condeelis, 2001), was much faster than that of control MDCK cells, which express no endogenous protein. In contrast, the traffic of vesicles, constitutive and stimulated, to and from the plasma membrane, was apparently unchanged in both MDCK and N2A cells expressing the wt α-synuclein. Taken together, these results suggest the participation of wt α-synuclein in the physiological regulation of the cytoskeleton remodeling taking place in some key processes, such as neurite outgrowth and adhesion of brain cells (Takenouchi *et al.,* 2001; Park *et al.,* 2002; Larsen *et al.,* 2006). In other processes, such as exo- and endocytosis, the role of the protein appears less important.

The actin-binding and modulation properties of wt α-synuclein discussed so far were substantially different from those exhibited by the A30P α-synuclein mutant. In the cell-free system, only the increased thickening of the filaments, due to the bundling activity of both α-synuclein forms, appeared similar. The other effects were different or opposite, a result that excludes our findings to be largely unspecific, dependent on an interaction with actin via structural properties conserved in the wt and mutant α-synuclein. With A30P α-synuclein actin polymerization at low $[Ca^{2+}]$ was faster than that of controls, an effect only partially reduced at high $[Ca^{2+}]$. A30P α-synuclein appeared to interact preferentially with actin filaments rather than monomers, in apparent agreement with the stabilization effect also exhibited by the mutant. The A30P mutation might therefore induce an alteration of the general conformation of α-synuclein, responsible for the substantial change of its binding to actin revealed by our results. Indeed, a conformational change has also been proposed to account for the differential effects of α-synucleins on microtubule assembly (Alim *et al.,* 2004).

Cytoskeletal alterations induced by A30P α-synuclein were visible in resting N2A but not in resting MDCK cells, which exhibited a normal phenotype. However this difference was probably only apparent, dependent on the distinct levels of expression of the mutant protein in the two cell types (5–6 and 2 μM, respectively). On LatA treatment, in fact, the cytoskeleton of both cells underwent a profound disorganization, particularly evident during recovery, with the appearance of numerous discrete foci composed by a dense actin shell surrounding an A30P α-synuclein core. In neurons these structures appeared as small structures, distributed especially along the neurites and at their terminal tips. These foci, attached to and rolling onto the inner face of the plasma membrane, especially near the sites of cell-to-cell interaction, appear as transient but specific structures, quite different from the protein clusters close to the plasma membrane recently reported in yeast cells overexpressing α-synuclein-GFP (Soper *et al.,* 2008).

The appearance of foci upon LatA-induced depolymerization of the cytoskeleton could be explained based on the properties of α-synuclein, an intrinsically unfolded protein with a tendency to aggregate which is greatly increased by the A30P mutation (Weinreb *et al.,* 1996; Uversky, 2003). Once released from actin filaments, in fact, A30P α-synuclein could aggregate into discrete cores serving as preferential sites for fast actin polymerization. Moreover, the apparent change in cell size noticed in N2A cells after LatA washout may indicate that A30P α-synuclein, and possibly the actin foci induced by its presence, interferes with the process of reextension of actin filaments necessary to maintain and to regain the cell shape. The subsequent reorganization of the cytoskeleton in A30P α-synuclein–expressing cells, although slower, was enough to disassemble the actin coat and induce the disappearance of foci.

Figure 10 (cont). close to the cell bodies of neurons expressing either exogenous wt or A30P α-synuclein, treated with LatA for 1 h, and fixed after a 1-h recovery. Notice the appreciable increase of the area and the formation of lamellipodia-like structures (asterisks) in the wt α-synuclein neuron and the areas of actin enrichment along the neurites (arrowheads) in the A30P α-synuclein neuron. (C) Statistical analysis of the average length (± SD) of minor and major neurites in embryonic hippocampal neurons electroporated either with an empty vector (CTRL) or with the constructs coding for wt or A30P α-synuclein (□, ▨, and ■, respectively). The minor neurites of the wt α-synuclein–expressing neurons are moderately longer, and the major neurites are shorter, and A30P α-synuclein expressing neurons display a significant decrease of the length of the major neurite. (D) Statistical analysis of the mean cell body area in CTRL, wt α-synuclein, and A30P α-synuclein–loaded embryonic hippocampal neurons, either untreated (NO LatA) or treated with LatA followed or not by recovery. After recovery (LatA rec 1 h, LatA rec 2 h), wt α-synuclein–expressing neurons display a significant increase in the cell body area, compared with CTRL and A30P α-synuclein–expressing neurons. (E) Statistical analysis of the average number of actin foci per neurite (± SD) in CTRL, wt, or A30P α-synuclein–expressing embryonic hippocampal neurons, either untreated (NO LatA) or treated with LatA followed or not by recovery. In A30P α-synuclein neurons the number of actin foci is significantly increased after LatA treatment (LatA) and during the actin cytoskeleton recovery (LatA rec 1 h). (F) Anti-actin immunoprecipitate obtained from the final supernatant isolated from a rat brain homogenate cleared with 1% Triton X-100 and centrifuged at 355,000 × *g* for 40 min. Actin coimmunoprecipitated endogenous α-synuclein. In the lane labeled FS, 2% of the brain final supernatant was loaded. In Ab, 0.2 μg of the anti-actin antibody was loaded as an internal reference. Statistical analysis in C–E was performed on 40 different images from three experiments. In C–E; * $p < 0.05$ and ** $p < 0.01$. Bars, (B and C) 20 μm.

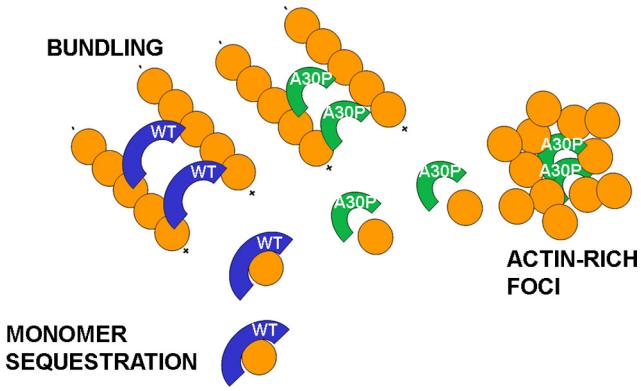

Figure 11. Hypothetical model of α-synuclein mechanisms of action on the actin cytoskeleton. According to the proposed model, both α-synucleins exert an actin bundling activity. However, only wt α-synuclein sequesters actin monomers. In contrast, A30P α-synuclein induces the formation of actin-rich foci around an A30P α-synuclein core. Blue arches, wt α-synuclein; green arches, A30P α-synuclein.

The cells expressing A30P α-synuclein were quite different from controls and from those expressing the wt protein also in the functional experiments. In the migration test, in fact, the A30P α-synuclein–rich cells were almost immobile; the constitutive membrane traffic to and from the plasma membrane was larger in both MDCK and N2A cells; however, the responses to ATP and high K^+ stimulation were completely ineffective or only weak, respectively. The membrane traffic results could be related to the disruption in the A30P α-synuclein–expressing cells of the actin barrier below the plasma membrane (Soldati and Schliwa, 2006). This structure, in fact, appears to decrease the probability of spontaneous vesicle exocytosis in resting cells. Its disruption, with the ensuing partial depletion of the intracellular pool of vesicles available for regulated exo- and endocytosis could be responsible for the decreased response observed upon stimulation.

Experiments carried out in primary cultures of hippocampal neurons document the relevance of our results also for neuronal cells. In addition, by studying neurons we obtained specific results concerning the sprouting of neurite processes, among which one, destined to grow as the axon, becomes rapidly longer than the others (Dotti *et al.*, 1988). With wt α-synuclein the elongation of minor neurites was increased, possibly because the sequestration of actin monomers was increasing actin fiber instability. In contrast the major neurite, especially in the case of A30P α-synuclein–expressing neurons, was shorter than that of controls.

In conclusion, our cell-free assays and whole cell results have revealed a novel mechanism of α-synuclein action, based on the binding to actin that appears profoundly different with the wt and the mutated protein. The model shown in Figure 11 illustrates the hypothetical mechanisms of action of the two α-synucleins. Wt α-synuclein acts as a monomer sequestering protein, able also to induce the formation of thin bundles possibly interacting with actin at two different binding sites. A30P α-synuclein, which has lost the capacity to bind actin monomers, binds actin filaments and stabilizes them. Moreover it is possible that, during actin remodeling, small aggregates of A30P α-synuclein assemble favoring the formation of transient actin-rich foci and the disorder of the whole actin organization. The structural and functional modulation of the cytoskeleton by wt α-synuclein and the profound disorder induced by A30P α-synuclein can be highly important for both the physiology and pathology of nerve cells. Wt α-synuclein might play an important role in the cytoskeletal reorganization taking place in a variety of conditions, for example, during the neuronal responses following axonal trauma (Quilty *et al.*, 2003), whereas the alterations induced by A30P α-synuclein could participate in the development of PD and other α-synuclein–dependent diseases.

ACKNOWLEDGMENTS

V.L.S. was a recipient of a postdoctoral fellowship from the Fundação para a Ciência e a Tecnologia, Portugal. M.Y. was a TRIL fellow of the Abdus Salam International Centre of Theoretical Physics, Trieste. We thank Stefano Maglie for his help with some of the experiments, Paola Podini for her contribution of electron microscopy, Daniela Talarico for suggestions on neuronal cultures, Eugenio Fornasiero for his help with interpretation of the data, Brett Lauring (Columbia University, New York, NY) for the gift of Syn constructs, Yukiko Goda (University College London, London, United Kingdom) for the actin-GFP construct and Daniele Zacchetti (San Raffaele Scientific Institute, Milan, Italy) for the MDCK inducible system. This work was founded in part by grants from the European Community (APOPIS-LSHM-CT-2003-503330), the Italian Ministry of Research (FIRB 2004 and PRIN 2006 Programs), the Telethon Fondazione Onlus (GGGP030234), and the CARIPLO Foundation (2006-0779).

REFERENCES

Abeliovich, A., *et al.* (2000). Mice lacking alpha-synuclein display functional deficits in the nigrostriatal dopamine system. Neuron *25*, 239–252.

Alim, M. A., *et al.* (2004).Demonstration of a role for alpha-synuclein as a functional microtubule-associated protein. J. Alzheimers Dis. *6*, 435–442; discussion 443–439.

Angleson, J. K., and Betz, W. J. (1997). Monitoring secretion in real time: capacitance, amperometry and fluorescence compared. Trends Neurosci. *20*, 281–287.

Banker, G. A., and Cowan, W. M. (1977). Rat hippocampal neurons in dispersed cell culture. Brain Res. *126*, 397–425.

Bertrand, C. A., Laboisse, C., Hopfer, U., Bridges, R. J., and Frizzell, R. A. (2006). Methods for detecting internalized, FM 1-43 stained particles in epithelial cells and monolayers. Biophys. J. *91*, 3872–3883.

Bradke, F., and Dotti, C. G. (1999). The role of local actin instability in axon formation. Science *283*, 1931–1934.

Cabin, D. E., *et al.* (2002). Synaptic vesicle depletion correlates with attenuated synaptic responses to prolonged repetitive stimulation in mice lacking alpha-synuclein. J. Neurosci. *22*, 8797–8807.

Chandra, S., *et al.* (2004). Double-knockout mice for alpha- and beta-synucleins: effect on synaptic functions. Proc. Natl. Acad. Sci. USA *101*, 14966–14971.

Chandra, S., Gallardo, G., Fernandez-Chacon, R., Schluter, O. M., and Sudhof, T. C. (2005). Alpha-synuclein cooperates with CSPalpha in preventing neurodegeneration. Cell *123*, 383–396.

Cheong, K. H., Zacchetti, D., Schneeberger, E. E., and Simons, K. (1999). VIP17/MAL, a lipid raft-associated protein, is involved in apical transport in MDCK cells. Proc. Natl. Acad. Sci. USA *96*, 6241–6248.

Chieregatti, E., Ceccaldi, P. E., Benfenati, F., and Valtorta, F. (1996). Effects of synaptic vesicles on actin polymerization. FEBS Lett. *398*, 211–216.

Condeelis, J. (2001). How is actin polymerization nucleated in vivo? Trends Cell Biol. *11*, 288–293.

Dawson, T. M., and Dawson, V. L. (2003). Rare genetic mutations shed light on the pathogenesis of Parkinson disease. J. Clin. Invest. *111*, 145–151.

Dillon, C., and Goda, Y. (2005). The actin cytoskeleton: integrating form and function at the synapse. Annu. Rev. Neurosci. *28*, 25–55.

Dotti, C. G., Sullivan, C. A., and Banker, G. A. (1988). The establishment of polarity by hippocampal neurons in culture. J. Neurosci. *8*, 1454–1468.

Esposito, A., Dohm, C. P., Kermer, P., Bahr, M., and Wouters, F. S. (2007). alpha-Synuclein and its disease-related mutants interact differentially with the microtubule protein tau and associate with the actin cytoskeleton. Neurobiol. Dis. *26*, 521–531.

Fortin, D. L., Nemani, V. M., Voglmaier, S. M., Anthony, M. D., Ryan, T. A., and Edwards, R. H. (2005). Neural activity controls the synaptic accumulation of alpha-synuclein. J. Neurosci. *25*, 10913–10921.

Gartner, A., Collin, L., and Lalli, G. (2006). Nucleofection of primary neurons. Methods Enzymol. *406*, 374–388.

Ichibangase, T., Saimaru, H., Takamura, N., Kuwahara, T., Koyama, A., Iwatsubo, T., and Imai, K. (2008). Proteomics of *Caenorhabditis elegans* overexpressing human alpha-synuclein analyzed by fluorogenic derivatization-liquid chromatography/tandem mass spectrometry: identification of actin and several ribosomal proteins as negative markers at early Parkinson's disease stages. Biomed. Chromatogr. *22*, 232–234.

Kahle, P. J., Neumann, M., Ozmen, L., and Haass, C. (2000). Physiology and pathophysiology of alpha-synuclein. Cell culture and transgenic animal models based on a Parkinson's disease-associated protein. Ann. NY Acad. Sci. *920*, 33–41.

Kruger, R., Kuhn, W., Muller, T., Woitalla, D., Graeber, M., Kosel, S., Przuntek, H., Epplen, J. T., Schols, L., and Riess, O. (1998). Ala30Pro mutation in the gene encoding alpha-synuclein in Parkinson's disease. Nat. Genet. *18*, 106–108.

Larsen, K. E., *et al.* (2006). Alpha-synuclein overexpression in PC12 and chromaffin cells impairs catecholamine release by interfering with a late step in exocytosis. J. Neurosci. *26*, 11915–11922.

Lesuisse, C., and Martin, L. J. (2002). Long-term culture of mouse cortical neurons as a model for neuronal development, aging, and death. J. Neurobiol. *51*, 9–23.

Liu, S., Ninan, I., Antonova, I., Battaglia, F., Trinchese, F., Narasanna, A., Kolodilov, N., Dauer, W., Hawkins, R. D., and Arancio, O. (2004). alpha-Synuclein produces a long-lasting increase in neurotransmitter release. EMBO J. *23*, 4506–4516.

Llorente, A., van Deurs, B., Garred, O., Eker, P., and Sandvig, K. (2000). Apical endocytosis of ricin in MDCK cells is regulated by the cyclooxygenase pathway. J. Cell Sci. *113*(Pt 7), 1213–1221.

Lucking, C. B., and Brice, A. (2000). Alpha-synuclein and Parkinson's disease. Cell Mol. Life Sci. *57*, 1894–1908.

MacLean-Fletcher, S., and Pollard, T. D. (1980). Identification of a factor in conventional muscle actin preparations which inhibits actin filament self-association. Biochem. Biophys. Res. Commun. *96*, 18–27.

Martinez, J., Moeller, I., Erdjument-Bromage, H., Tempst, P., and Lauring, B. (2003). Parkinson's disease-associated alpha-synuclein is a calmodulin substrate. J. Biol. Chem. *278*, 17379–17387.

McCarthy, K. M., Skare, I. B., Stankewich, M. C., Furuse, M., Tsukita, S., Rogers, R. A., Lynch, R. D., and Schneeberger, E. E. (1996). Occludin is a functional component of the tight junction. J. Cell Sci. *109*(Pt 9), 2287–2298.

Meijering, E., Jacob, M., Sarria, J. C., Steiner, P., Hirling, H., and Unser, M. (2004). Design and validation of a tool for neurite tracing and analysis in fluorescence microscopy images. Cytometry A *58*, 167–176.

Nakajo, S., Tsukada, K., Kameyama, H., Furuyama, Y., and Nakaya, K. (1996). Distribution of phosphoneuroprotein 14 (PNP 14) in vertebrates: its levels as determined by enzyme immunoassay. Brain Res. *741*, 180–184.

Nielsen, M. S., Vorum, H., Lindersson, E., and Jensen, P. H. (2001). Ca^{2+} binding to alpha-synuclein regulates ligand binding and oligomerization. J. Biol. Chem. *276*, 22680–22684.

Park, S. M., Jung, H. Y., Kim, H. O., Rhim, H., Paik, S. R., Chung, K. C., Park, J. H., and Kim, J. (2002). Evidence that alpha-synuclein functions as a negative regulator of Ca(++)-dependent alpha-granule release from human platelets. Blood *100*, 2506–2514.

Peng, X., Tehranian, R., Dietrich, P., Stefanis, L., and Perez, R. G. (2005). Alpha-synuclein activation of protein phosphatase 2A reduces tyrosine hydroxylase phosphorylation in dopaminergic cells. J. Cell Sci. *118*, 3523–3530.

Quilty, M. C., Gai, W. P., Pountney, D. L., West, A. K., and Vickers, J. C. (2003). Localization of alpha-, beta-, and gamma-synuclein during neuronal development and alterations associated with the neuronal response to axonal trauma. Exp. Neurol. *182*, 195–207.

Shibayama-Imazu, T., Okahashi, I., Omata, K., Nakajo, S., Ochiai, H., Nakai, Y., Hama, T., Nakamura, Y., and Nakaya, K. (1993). Cell and tissue distribution and developmental change of neuron specific 14 kDa protein (phosphoneuroprotein 14). Brain Res. *622*, 17–25.

Singleton, A. B., *et al.* (2003). alpha-Synuclein locus triplication causes Parkinson's disease. Science *302*, 841

Soldati, T., and Schliwa, M. (2006). Powering membrane traffic in endocytosis and recycling. Nat. Rev. Mol. Cell Biol. *7*, 897–908.

Soper, J. H., Roy, S., Stieber, A., Lee, E., Wilson, R. B., Trojanowski, J. Q., Burd, C. G., and Lee, V. M. (2008). α-Synuclein-induced Aggregation of Cytoplasmic Vesicles in *Saccharomyces cerevisiae*. Mol. Biol. Cell *19*, 1093–1103.

Specht, C. G., and Schoepfer, R. (2001). Deletion of the alpha-synuclein locus in a subpopulation of C57BL/6J inbred mice. BMC Neurosci. *2*, 11.

Spector, I., Braet, F., Shochet, N. R., and Bubb, M. R. (1999). New anti-actin drugs in the study of the organization and function of the actin cytoskeleton. Microsc. Res. Tech. *47*, 18–37.

Spudich, J. A., and Watt, S. (1971). The regulation of rabbit skeletal muscle contraction. I. Biochemical studies of the interaction of the tropomyosin-troponin complex with actin and the proteolytic fragments of myosin. J. Biol. Chem. *246*, 4866–4871.

Takenouchi, T., Hashimoto, M., Hsu, L. J., Mackowski, B., Rockenstein, E., Mallory, M., and Masliah, E. (2001). Reduced neuritic outgrowth and cell adhesion in neuronal cells transfected with human alpha-synuclein. Mol. Cell Neurosci. *17*, 141–150.

Tao-Cheng, J. H. (2006). Activity-related redistribution of presynaptic proteins at the active zone. Neuroscience *141*, 1217–1224.

Totterdell, S., Hanger, D., and Meredith, G. E. (2004). The ultrastructural distribution of alpha-synuclein-like protein in normal mouse brain. Brain Res. *1004*, 61–72.

Tsuboi, K., Grzesiak, J. J., Bouvet, M., Hashimoto, M., Masliah, E., and Shults, C. W. (2005). Alpha-synuclein overexpression in oligodendrocytic cells results in impaired adhesion to fibronectin and cell death. Mol. Cell Neurosci. *29*, 259–268.

Uversky, V. N. (2003). A protein-chameleon: conformational plasticity of alpha-synuclein, a disordered protein involved in neurodegenerative disorders. J. Biomol. Struct. Dyn. *21*, 211–234.

Walev, I., Bhakdi, S. C., Hofmann, F., Djonder, N., Valeva, A., Aktories, K., and Bhakdi, S. (2001). Delivery of proteins into living cells by reversible membrane permeabilization with streptolysin-O. Proc. Natl. Acad. Sci. USA *98*, 3185–3190.

Weinreb, P. H., Zhen, W., Poon, A. W., Conway, K. A., and Lansbury, P. T., Jr. (1996). NACP, a protein implicated in Alzheimer's disease and learning, is natively unfolded. Biochemistry *35*, 13709–13715.

Xun, Z., Sowell, R. A., Kaufman, T. C., and Clemmer, D. E. (2007). Protein expression in a *Drosophila* model of Parkinson's disease. J. Proteome Res. *6*, 348–357.

Yamazaki, D., Oikawa, T., and Takenawa, T. (2007). Rac-WAVE-mediated actin reorganization is required for organization and maintenance of cell-cell adhesion. J. Cell Sci. *120*, 86–100.

Zhou, Y., Gu, G., Goodlett, D. R., Zhang, T., Pan, C., Montine, T. J., Montine, K. S., Aebersold, R. H., and Zhang, J. (2004). Analysis of alpha-synuclein-associated proteins by quantitative proteomics. J. Biol. Chem. *279*, 39155–39164.